Structural stability of lithium manganese oxides

S. K. Mishra and G. Ceder
Department of Materials Science & Engineering, Massachusetts Institute of Technology, 77 Massachusetts Avenue, Cambridge, Massachusetts 02139
(Received 6 October 1998)

We have studied stability of lithium-manganese oxides using density functional theory in the local density and generalized gradient approximation (GGA). In particular, the effect of spin-polarization and magnetic ordering on the relative stability of various structures is investigated. At all lithium compositions the effect of spin polarization is large, although it does not affect different structures to the same extent. At composition $LiMnO_2$, globally stable Jahn-Teller distortions could only be obtained in the spin-polarized GGA approximation, and antiferromagnetic spin ordering was critical to reproduce the orthorhombic $LiMnO_2$ structure as ground state. We also investigate the effect of magnetism on the Li intercalation potential, an important property for rechargeable Li batteries. [S0163-1829(99)00709-2]

I. INTRODUCTION

Lithiated manganese oxides are of considerable technological and scientific interest.[1–4] Several of the Mn-oxide crystal types can accomodate Li ions to large composition. These materials can therefore be applied on the cathode side of a rechargeable Li battery where Li is stored during the discharge cycle of the battery. Reversibility of Li insertion and removal into the manganese oxide host is necessary to ensure multiple charge and discharge cycles. Because of its low cost and limited environmental impact, lithium manganese oxide has the potential to replace $LiCoO_2$ as the material of choice in rechargeable batteries.[4,5]

Lithiated manganese oxides are also interesting from a more basic viewpoint. The manganese cation is typically high spin with a very large magnetic moment. Mn^{3+} is a prototypical Jahn-Teller ion, giving rise to a tetragonal deformation of the oxygen environment around it (e.g., $LaMnO_3$).[6,7] Since lithium is fully ionized to Li^+ in these oxides,[8] charge neutrality requires that insertion or removal of Li from the structure is accompanied by electron transfer to and from the manganese-oxide host, changing the effective valence state of the Mn ion. While the Mn ion in MnO_2 is believed to have the electronic configuration t_{2g}^3-e_g^0, lithiation up to $LiMnO_2$ leads to occupation of the doubly degenerate e_g level. In octahedral symmetry the two e_g orbitals consist of an antibonding combination of the $3d_{z^2}/3d_{x^2-y^2}$ and oxygen p orbitals, so that their occupation leads to an increase in the oxygen-metal bond length. In one type of Jahn-Teller (JT) distortion, the symmetry between the occupied and empty level is spontaneously broken by an increase in two of the metal-oxygen bonds along the $3d_{z^2}$ orbital. Although Mn^{3+} is almost always a JT ion and Mn^{4+} never is, disagreement exists what average valence is required to cause a JT distortion in structures with mixtures of Mn^{3+} and Mn^{4+}. In $LiMn_2O_4$ where the average valence of Mn is 3.5, a tetragonal unit cell distortion has been found below room temperature,[9] with the cubic-tetragonal transition temperature being very dependent on Li (Ref. 10) and oxygen stoichiometry.[11,12] While the c/a ratio of this unit cell is only about 1.01, an extended x-ray absorption fine structure (EXAFS) study by Yamaguchi *et al.*[13] showed that the distortion of the local octahedral symmetry around Mn is much larger and of the order of 20%. Recently a charge ordered phase has been characterized by neutron and electron diffraction.[14]

While manganese oxides can exist in a variety of structures, this work will be limited to those that are relevant for Li insertion reactions. At composition $LiMn_2O_4$, the cubic spinel structure is the stable phase[5,15] with tetragonal[9] and orthorhombic[14,16–18] deformations possible at low temperature. The description of various structures are listed in Table I. The cubic spinel $LiMn_2O_4$ has space group $Fd\bar{3}m$ with the Mn and Li cations, respectively, on the $16(d)$ and $8(a)$ sites and the oxygen ions on the $32(e)$ site. The tetragonal spinel has been described in the $I4_1/amd$ (D_{4h}^{19}) (No. 141) space group with Mn and Li on the $8(d)$ and $4(a)$ sites, respectively, and the oxygen on the $16(h)$ site. Although for higher Li content ($LiMnO_2$) an orthorhombic structure (space group $Pmmn$) is the ground state,[19,20] lithiation of the spinel always leads to a phase in which the Mn cations retain the $16(d)$ sites of the spinel but the Li ions occupy the other octahedral sites $16(c)$. To illustrate its relation to the spinel we will always write the stoichiometry of this phase as $Li_2Mn_2O_4$. The Mn-O framework of spinel is tetragonally distorted due to the JT effect and the space group is lowered from $Fd\bar{3}m$ to $I4_1/amd$ (D_{4h}^{19}). Neutron diffraction on electrochemically lithiated spinels[21] shows that this ''ideal'' cation distribution is not achieved and a substantial amount of Li ions remain in the tetrahedral $8(a)$ sites of the starting spinel material.

Besides the orthorhombic and spinel structure, a layered $LiMnO_2$ with space group $C2/m$ was recently synthesized.[22,23] This structure is similar to the α-$NaFeO_2$ structure of $LiCoO_2$ and $LiNiO_2$ but with a monoclinic distortion induced by the JT effect on Mn^{3+}. While pure $LiMnO_2$ has only been synthesized in the monoclinic layered form by ion-exchange from $NaMnO_2$,[22–24] or by *in situ* ion exchange in KOH mixtures,[25] Al-doped layered Mn oxides can be directly synthesized from the hydroxides.[26]

TABLE I. The crystal structures and the ionic positions for lithiated manganese oxide.

Structure	Space group	Li site	Mn site	O site	Jahn-Teller distortion Possible ?
LA (Layered)	$R\bar{3}m$	3b	3a	6c	No
MLA (Monoclinic Layered)	$C/2m$	2d	2a	4i	Yes
SPC (Cubic Spinel) ($LiMn_2O_4$)	$Fd\bar{3}m$	8a	16d	32e	No
SPC (Cubic Spinel) ($Li_2Mn_2O_4$)	$Fd\bar{3}m$	16c	16d	32e	No
SPT (Tetragonal Spinel) ($LiMn_2O_4$)	$I4_1/amd$	8d	4a	16h	Yes
SPT (Tetragonal Spinel) ($Li_2Mn_2O_4$)	$I4_1/amd$	8d	8c	16h	Yes
ORTHO (Orthorhombic)	$Pmmn$	2a	2a	O1: 2b O2: 2b	Yes

Given the various possibilities of metastable structures that can be synthesized, a systematic study of the phase stabilities of the structures is useful. In this paper, we calculate the total energies of layered, orthorhombic, and spinel-based manganese oxides, with and without lithium ions. For the lithiated materials the distorted variants of these structures (monoclinic layered and tetragonal spinel) are also calculated. Exchange-correlation corrections are treated in both the local density approximation (LDA) and the generalized gradient approximation (GGA). Because of the high spin nature of the Mn cation, both spin polarized and non-spin-polarized calculations are presented. While spin polarization is essential to induce the JT distortion, it does not affect all structures in the same way and significantly favors the spinel-based structures, thereby leading to qualitative changes in the relative stability of the structures. At composition $LiMnO_2$ antiferromagnetic spin ordering is essential to obtain the correct ground state.

The enhanced localization offered by the GGA over the LDA is found critical to obtain the correct relative stability of the various structures. This is largely due to the fact that within the LDA the JT distortions are metastable or unstable.

Finally, we investigate the average potential at which Li can be inserted in the various structures and discuss its relation to the magnetic state of the Mn ion. Our results show that spin polarization affects the Li insertion voltage somewhat (≈ 0.3 V). The effect of the JT distortion is more variable.

II. METHODOLOGY

All total energies are obtained in the local density approximation and generalized gradient approximation to density functional theory as implemented in the VASP program.[27–29] Ultrasoft pseudopotentials are used to describe the effect of the nucleus and core electrons in the valence states. The valence electrons wave functions are expanded in plane waves. For the expansion of plane waves an energy cutoff of 600 eV was used for manganese oxides and metallic lithium. The reciprocal space sampling was done with 27 to 83 k points (depending on the structure) for the oxide and 256 k points for metallic lithium in the irreducible Brillouin zone. Both the volume and ionic positions were relaxed during the self-consistent energy minimization. The spin-polarized calculations are performed with both ferromagnetic (FM) and antiferromagnetic (AF) arrangements of the spin on the Mn ions. The application of pseudopotential techniques is now well established for oxides and has previously been applied to lithium-transition metal oxides[8,30–34] with the results in good agreement with all-electron full-potential linear augmented-plane-wave (FLAPW) calculations on the same materials.[35]

Total energy calculations can be related to the average Li insertion potential between two compositions limits by methods previously established.[8,30,31] If ΔG_r is the Gibbs free energy (in J/m) for the reaction:

$$MnO_2(\text{cathode}) + Li(\text{anode}) \rightarrow LiMnO_2(\text{cathode}) \quad (1)$$

the average insertion voltage is given by

$$\bar{V} = -\frac{\Delta G_r}{F}, \quad (2)$$

where F is the Faraday constant. Although the above equations imply metallic Li as the standard state for the Li potential, insertion voltages with respect to other anodes can be easily obtained by combining the results with the appropriate anode reaction energies. The energy of Li metal is calculated in the bcc structure. Since the effects due to change in volume and entropy is very small, the change in Gibbs free energy $\Delta G_r (\equiv \Delta E_r + P\Delta V_r - T\Delta S_r)$ can be approximated by only the change in the internal energy (ΔE_r) at 0 K. This approximation has been further verified by recent first-principles calculation which indicated that the difference between ΔE at 0 K and at 300 K is only ~ 30 meV.[36]

III. RESULTS

A. Non-spin-polarized (LDA)

The calculated lattice parameters and energies for the non-spin-polarized case with LDA are listed in Table II. The relative stability of all the structures is shown in Fig. 1(a). In Fig. 1(a) we have plotted the formation energy, defined as

$$\Delta E_f(Li_xMnO_2) = E_{Li_xMnO_2} - xE_{LiMnO_2}(\text{layered}) - (1-x)E_{MnO_2}(\text{layered}). \quad (3)$$

For $x=0$ or $x=1$, a negative ΔE_f indicates that the compound is more stable than layered MnO_2 and $LiMnO_2$, respectively. For $0<x<1$ a negative formation energy indi-

TABLE II. The energies and lattice parameters of various structures optimized without spin polarization effect in the local density approximation. The various structures are layered (LA), monoclinic layered (MLA), cubic spinel (SPC), tetragonal spinel (SPT), and orthorhombic (ORTHO). Energies are defined with respect to the concentration weighted average of MnO_2 and $LiMnO_2$ in the LA structure. The experimentally measured parameters are given in Table III.

Composition	Structure	a (Å)	b (Å)	c (Å)	β	Internal parameter	d(Mn-O) (Å)	ΔE_f (meV)
MnO_2	LA	2.74	2.74	13.45	90°	$x=0.262$	1.86	0.0
	MLA					relaxed to LA		
	SPC	7.85	7.85	7.85	90°	$x=0.389$	1.86	41
	SPT					relaxed to SPC		
	ORTHO	2.85	3.62	5.53	90°	Mn: $z=0.680$	1.71,1.88,2.03	−263
						O1: $z=0.148$		
						O2: $z=0.582$		
$Li_{0.5}MnO_2$	SPC	7.84	7.84	7.84	90°	$x=0.384$	1.89	−232
	SPT					relaxed to SPC		
$LiMnO_2$	LA	2.67	2.67	14.59	90°	$x=0.254$	1.93	0.0
	MLA					relaxed to LA		
	ORTHO	2.63	3.84	6.03	90°	Li: $z=0.089$	1.87,1.94,1.98	264
						Mn: $z=0.644$		
						O1: $z=0.136$		
						O2: $z=0.602$		
$Li_2Mn_2O_4$	SPC	7.84	7.84	7.84	90°	$x=0.379$	1.94	107
	SPT					relaxed to SPC		

cates that the material is stable with respect to phase separation into MnO_2 and $LiMnO_2$. The choice of the layered phases as reference states for the energy is arbitrary and does not affect any conclusions.

The orthorhombic and the layered structures have the lowest energy at MnO_2 and $LiMnO_2$ stoichiometries, respectively, while the unlithiated and fully lithiated spinel-based structures are higher in energy. The stoichiometric spinel ($LiMn_2O_4$) is stable with respect to phase separation. No stable JT distortions were obtained. Both the monoclinic layered and the tetragonal spinels relaxed back to their undeformed counterparts.

B. Spin-polarized (LDA)

1. Ferromagnetic ordering

The relative stability of various structures changes significantly when the spin polarization effect is included, as shown in Fig. 1(b). The corresponding lattice parameters are listed in Table III. The formation energy in Fig. 1(b) is again defined by Eq. (3), but now with respect to the spin-polarized layered phases. The strong magnetic moment on Mn reduces the energy of the MnO_2, $Li_{0.5}MnO_2$, and $Li_2Mn_2O_4$ spinels by, respectively, 800, 900, and 610 meV. The spin polarization effect also alters the relative stability of the structures. In fact, the magnetic effect reverses the order of some structures in terms of energetic stability. At MnO_2 composition, the layered structure is now the ground state with energy well below the orthorhombic structure. The spinel structure is higher in energy than the layered one. No stable JT distortions were found at this composition, as is to be expected for manganese with formal valence of $4+$. The spin polarization effect is again quite dramatic for the fully lithiated compounds where the formal valence of the Mn reduces to $3+$. Locally stable JT distortions could be found in the tetragonal spinel $LiMnO_2$ and in the monoclinic structure, but in each case the energy of the deformed structure was higher than for the undeformed one, so that the JT distortion is only *metastable*. The tetragonal deformation of the $Li_{0.5}MnO_2$ spinel was found to be unstable and relaxed back to the cubic symmetry.

2. Antiferromagnetic ordering

In the previous calculations, the magnetic moments on the Mn ions are aligned ferromagnetically so that the symmetry of the magnetic unit cell is the same as that based on the ionic positions. Recently, Singh[37] reported that, at the experimentally measured lattice parameters and ionic positions, the antiferromagnetic state of the monoclinic layered structure is lower in energy than the ferromagnetic one. For the orthorhombic $LiMnO_2$ structure[17] and the cubic $LiMn_2O_4$ spinel[38] antiferromagnetism has been observed experimentally. To investigate whether antiferromagnetism could further modify the relative stability at $LiMnO_2$, we calculated the energy of several structures with an antiferromagnetic (AF) arrangement of the Mn ions [Fig. 1(b) and Table IV]. Because of the constraints in computing resources we limited the AF calculations to composition $LiMnO_2$ and $Li_{0.5}MnO_2$. For the orthorhombic structure we considered the experimentally measured AF arrangements of the Mn ions.[17] For the monoclinic structure the antiferromagnetic ordering AF3 proposed by Singh[37] was considered. In both structures antiferromagnetic chains run along the direction of shortest Mn-Mn bonds. While for MLA and SPT an antiferromagnetic arrangement has lower energy than the corresponding ferromagnetic ones, this effect is not enough to make the de-

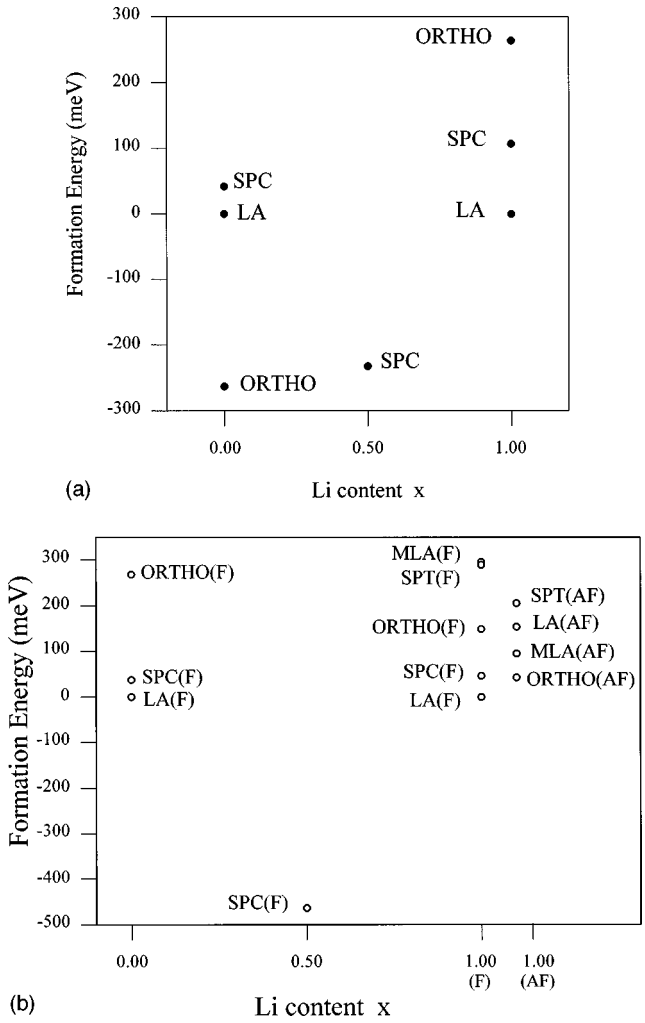

FIG. 1. The phase stability of various structure as a function of Li composition x calculated with LDA (a) for non-spin-polarized case and (b) for spin-polarized case.

formed AF structure stable over the undeformed FM ones and the ferromagnetic layered structure remains the overall ground state.

As is typical in the LDA, the optimized lattice parameters from our calculations are smaller than the experimental values. To investigate whether the JT distortions could be stabilized at higher volumes, we performed calculations for the material under negative pressure with both antiferromagnetic and ferromagnetic spin arrangements. We prefer the use of a negative pressure rather than fixing the volume at the experimental one, since this method allows for the unbiased comparison of various structures, even those for which no experimental data is available. Experimental lattice constants for the different structures were obtained for pressures in the range -30 kbar to -50 kbar. At these pressures the enthalpy of the Jahn-Teller distorted structure is slightly lower than that of the non-Jahn-Teller structures and the overall ground state is the antiferromagnetic orthorhombic structure.

In summary, the LDA fails to predict stable JT distortions. While it predicts several structures at composition $LiMnO_2$ to be antiferromagnetic the ground state is the ferromagnetic layered structure, in disagreement with experiments. Correcting the LDA volume by applying negative pressure does bring the results in closer agreement with experiments.

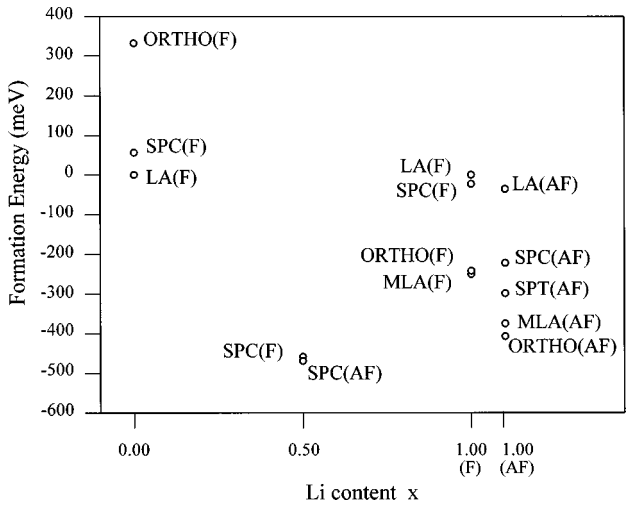

FIG. 2. The phase stability of various structure as a function of Li composition x calculated with GGA for spin-polarized case.

C. Spin polarized (GGA)

We also performed calculations for all structures in the generalized gradient approximation (GGA). Since the GGA usually leads to lattice parameters in closer agreement with experiment, we would expect it to give better results on Jahn-Teller distorted structures. In addition, the enhanced localization offered by the GGA should further stabilize the Jahn-Teller distortion. Volume and internal coordinates are relaxed to find the lowest energy. Since the effect of spin polarization was found to be essential we do not present any non-spin-polarized results. Ferromagnetic (FM) and antiferromagnetic (AF) arrangements of the Mn ions are considered. The AF arrangements are the same as for the LDA calculations. For composition MnO_2 only ferromagnetic states were calculated due to limited computing resources. The calculated parameters are listed in Table V. The GGA improves the lattice parameters and also makes the JT distorted structures more stable relative to the nondeformed ones (both for ferromagnetic and antiferromagnetic arrangements). For example, the monoclinic structure is now stable over the layered structure and the tetragonal spinel over the cubic spinel structure. For all the structures we calculated, AF spin ordering is stable over FM spin ordering. (We did not perform AF calculation at composition MnO_2.) The relative stabilities of various structures for Li_xMnO_2 at $x = 0, 0.5$, and 1 compositions are shown in Fig. 2. For the delithiated MnO_2 composition the layered structure remains most stable. The suspected tetragonal distortion in the spinel phase ($Li_{0.5}MnO_2$) (Ref. 9) still could not be obtained with GGA as the deformed structure relaxed back to the cubic spinel in our calculation. The recently proposed new ground state for this composition has too large an unit cell to be accessible with first-principle calculations.[14,16] The effect of the GGA coupled with magnetism is very dramatic at the fully lithiated $LiMnO_2$ composition. The antiferromagnetic orthorhombic structure is now the ground state which is consistent with experiment.[17] The orthorhombic (AF) is 32 meV

TABLE III. The energies and lattice parameters of various structures optimized with ferromagnetic spin polarization effect in the local density approximation. Experimentally known parameters are given in brackets.

Composition	Structure	a (Å)	b (Å)	c (Å)	β	Internal parameter	d(Mn-O) (Å)	ΔE_f (meV)
MnO_2	LA	2.84	2.84	13.15	90°	$x=0.262$	1.89	0
	MLA					relaxed to LA		
	SPC	7.96	7.96	7.96	90°	$x=0.388$	1.89	37
	SPT					relaxed to SPC		
		(8.04)	(8.04)	(8.04)	(90°)	(0.263)	(1.95)	(Ref. 15)
	ORTHO	2.81	3.73	5.63	90°	Mn: $z=0.669$	1.78,1.92,2.01	268
						O1: $z=0.137$		
						O2: $z=0.585$		
$Li_{0.5}MnO_2$	SPC	7.98	7.98	7.98	90°	$x=0.387$	1.91	464
		(8.24)	(8.24)	(8.24)	(90°)	($x=0.262$)	(1.96)	(Ref. 15)
	SPT					relaxed to SPC		
$LiMnO_2$	LA	2.77	2.77	14.11	90°	$x=0.257$	1.94	0
	MLA	5.35	2.78	5.27	116°	$x=0.269$, $z=0.768$	1.88,2.26	296
		(5.44)	(2.81)	(5.39)	(116°)	($x=0.272$, $z=0.771$)	(1.92,2.31)	(Ref. 22)
	ORTHO	2.76	4.16	5.73	90°	Li: $z=0.106$	1.89,1.96,2.08	149
						Mn: $z=0.630$		
						O1: $z=0.143$		
						O2: $z=0.611$		
		(2.81)	(4.57)	(5.76)	(90°)	(0.126,0.635)	(1.89,1.95,2.29)	(Ref. 20)
						(0.144,0.602)		
$Li_2Mn_2O_4$	SPC	7.92	7.92	7.92	90°	$x=0.380$	1.94	43
	SPT	5.59	5.59	9.15	90°	$x=0.482$, $z=0.248$	1.90,2.26	289
		(5.65)	(5.65)	(9.25)	(90°)	($x=0.485$, $z=0.253$)	(1.937,2.286)	(Ref. 9)

lower in energy than the monoclinic (AF). If only ferromagnetic spin ordering is allowed the stability is reversed, namely, the MLA (FM) is lower than the orthorhombic (FM) by 8 meV. This calculation reveals that antiferromagnetism is necessary to stabilize the orthorhombic structure over the monoclinic layered structure.

In summary, we find that the GGA can produce stable Jahn-Teller distortion in this system, in contrast to the LDA. The effect of spin ordering is relatively large, in the case of MLA and ORTHO even reversing their respective stability. For all structures investigated, we find that antiferromagnetism is stable over ferromagnetism.

D. Electronic structure

In $LiMnO_2$ compounds, the Mn ions are surrounded by six oxygen ions forming an octahedron. For a transition metal in octahedral symmetry, the d_{z^2} and $d_{x^2-y^2}$ atomic orbitals directly overlap with the p_x, p_y, and p_z orbitals of the oxygen along the octahedral directions. This σ overlap forms the e_g bands. For a highly ionic system the antibonding band $e_g^\star$ consists of mainly the metal d states, whereas the bonding e_g^b band is predominantly of oxygen p character. The remaining d_{xy}, d_{xz}, and d_{yz} orbitals point away from the O and have no σ overlap with its p orbitals. These orbitals form nonbonding t_{2g} bands. So in the octahedral crystal field, the d manifold splits into the lower t_{2g} and upper e_g states. In Fig. 3, we show the band structure for $LiMnO_2$ calculated with LDA in the layered structure (no JT distortion) at zero pressure along the high-symmetry directions of the Brillouin zone. The up and down spin part are plotted separately. Here we show only the LDA band structures because the band structures obtained from GGA exhibit similar

TABLE IV. The energies [with respect to LA(F)] and lattice parameters of various structures optimized with antiferromagnetic spin polarization effect in the local density approximation.

Composition	Structure	a (Å)	b (Å)	c (Å)	β	Internal parameter	d(Mn-O) (Å)	ΔE_f (meV)
	LA	2.86	2.86	13.20	90°	$x=0.267$	1.89,1.93	154
$LiMnO_2$	MLA	5.05	3.06	5.01	116°	$x=0.270$, $z=0.766$	1.89,1.91,2.26	96
	ORTHO	2.76	4.43	5.62	90°	Li: $z=0.115$	1.87,1.92,2.22	46
						Mn: $z=0.637$		
						O1: $z=0.137$		
						O2: $z=0.601$		
$Li_2Mn_2O_4$	SPT	5.57	5.57	8.94	90°	$x=0.482$, $z=0.246$	1.90,2.27	206

TABLE V. The energies and lattice parameters of various structures optimized with ferromagnetic and antiferromagnetic spin polarization effect in the generalized gradient approximation. Experimentally known parameters are given in brackets. The parameter β is 116° for the MLA structure and 90° for all other structures.

Composition	Structure	a (Å)	b (Å)	c (Å)	Internal parameter	d(Mn-O) (Å)	ΔE_f (meV)
MnO_2	LA(F)	2.90	2.90	15.82	$x=0.273$	1.93	0
	MLA(F)				relaxed to LA		
	SPC(F)	8.18	8.18	8.18	$x=0.390$	1.93	57
	SPT(F)				relaxed to SPC		
		(8.04)	(8.04)	(8.04)	(0.263)	(1.95)	(Ref. 15)
	ORTHO(F)	2.87	3.81	6.07	Mn: $z=0.660$	1.81,1.97,2.04	332
					O1: $z=0.158$		
					O2: $z=0.579$		
$Li_{0.5}MnO_2$	SPC(F)	8.12	8.12	8.12	$x=0.386$	1.94	−459
	SPT(F)				relaxed to SPC		
	SPT(AF)	5.89	5.89	8.04	$x=0.477,\ z=0.262$	1.92,1.99	−469
		(5.65)	(5.65)	(9.25)	($x=0.485,\ z=0.253$)	(1.937,2.286)	(Ref. 9)
$LiMnO_2$	LA(F)	2.82	2.82	14.27	$x=0.255$	1.97	0
	LA(AF)	2.90	2.90	13.63	$x=0.270$	1.90,1.95	−36
	MLA(F)	5.54	2.82	5.44	$x=0.270,\ z=0.763$	1.92,2.34	−248
		(5.44)	(2.81)	(5.39)	($x=0.272,\ z=0.771$)	(1.92,2.31)	(Ref. 22)
	MLA(AF)	5.54	2.77	5.47	$x=0.271,\ z=0.762$	1.92,1.93,2.39	−375
	ORTHO(F)	2.80	4.82	5.60	Li: $z=0.116$	1.91,1.95,2.32	−241
					Mn: $z=0.638$		
					O1: $z=0.128$		
					O2: $z=0.605$		
	ORTHO(AF)	2.79	4.69	5.64	Li: $z=0.104$	1.92,1.95,2.35	−407
					Mn: $z=0.636$		
					O1: $z=0.132$		
					O2: $z=0.606$		
		(2.81)	(4.57)	(5.76)	(0.126,0.635)	(1.89,1.95,2.29)	(Ref. 20)
					(0.144,0.602)		
$Li_2Mn_2O_4$	SPC(F)	8.38	8.38	8.38	$x=0.381$	2.04	−23
	SPC(AF)	5.82	5.82	8.21	$x=0.384$	1.91,2.00	−221
	SPT(AF)	5.61	5.61	9.52	$x=0.484,\ z=0.247$	1.93,2.39	−298
		(5.65)	(5.65)	(9.25)	($x=0.485,\ z=0.253$)	(1.937,2.286)	(Ref. 9)

features. The top two e_g bands are separated from the three t_{2g} bands by a gap of about 2.5 eV. The O($2p$) bands are below the Mn(d) bands and lie about 5 eV below the Fermi energy E_F. Clearly, Mn is not fully high spin as there is some occupation of the minority t_{2g} bands. To examine the effect of Li intercalation in the electronic structure, we compared the bands of lithiated $LiMnO_2$ with those of the delithiated MnO_2 (not shown). As Li is inserted into the host MnO_2 structure, the e_g bands shifts down and the lower portion of the O($2p$) bands are pushed up. Upon Li intercalation, the Mn-O bond length increases, thus reducing the σ overlap between the O($2p$) and Mn(d) orbitals. Hence the bonding bands are pushed up and the antibonding bands are pushed down. The effect of JT distortion can be seen in Figs. 4(a) and 4(b) where the band structure for $LiMnO_2$ with the monoclinic deformation under the negative pressure is plotted. The band structure is insulating with a small gap of about 120 meV. This is in good agreement with the results from FLAPW on the experimental geometry[37] and much smaller than the gap calculated in the Hartree-Fock approximation.[39] The minority spin Mn(d) bands [Fig. 4(b)] are all above the E_F indicating fully high spin Mn^{3+}. Both the minority and the majority bands are relatively flat over the entire range of the Brillouin zone. The high spin JT distorted Mn^{3+} ion splits the e_g bands, half of them being occupied. The spin polarized bands for $Li_2Mn_2O_4$ in the tetragonal spinel structure also exhibit similar features, as shown by the density of states plot in Fig. 5. For comparison the density of states for $LiMn_2O_4$ in the cubic spinel structure is plotted in Fig. 6. Clearly, the JT distortion is essential for obtaining a fully high spin Mn^{3+} ion. The O($2p$) bands are about 6 eV below the Fermi energy. As can be seen from Fig. 6, there is some overlap between the O($2p$) and the occupied majority Mn(t_{2g}) orbitals. There are few carriers in the minority Mn(t_{2g}) bands which barely crosses the Fermi level. The Mn(e_g) bands are all empty.

E. Intercalation voltage

For application in rechargeable Li batteries, the Li insertion potential is of interest. The average lithiation potential can be obtained from the energy of the Li_xMnO_2 compounds

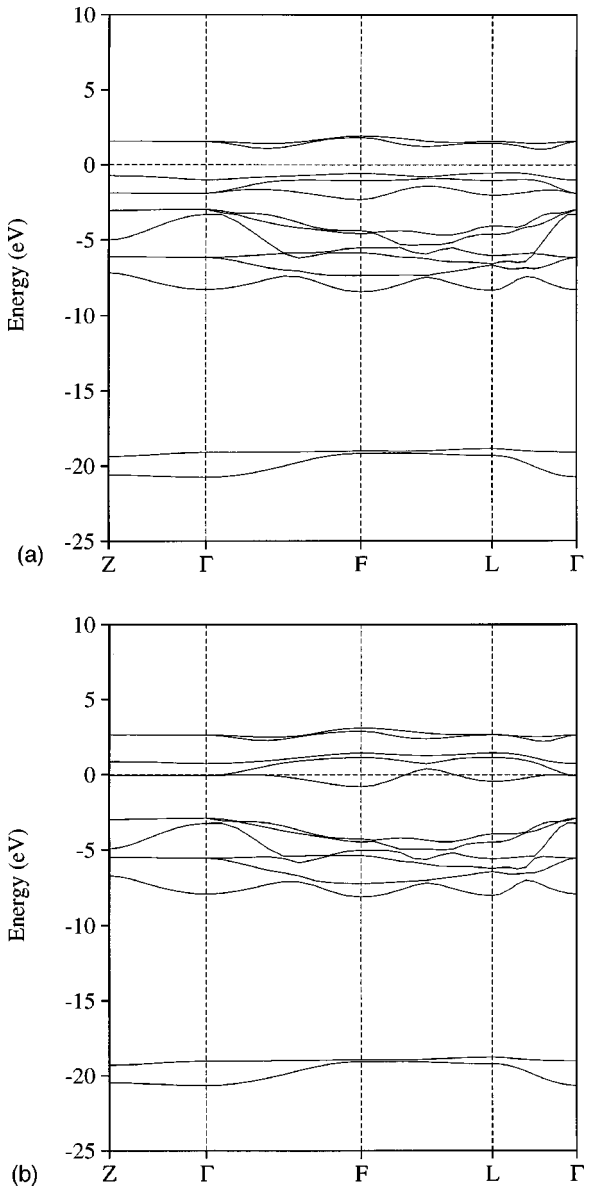

FIG. 3. The LDA band structures of $LiMnO_2$ in the layered structure (a) for the majority and (b) for the minority spin.

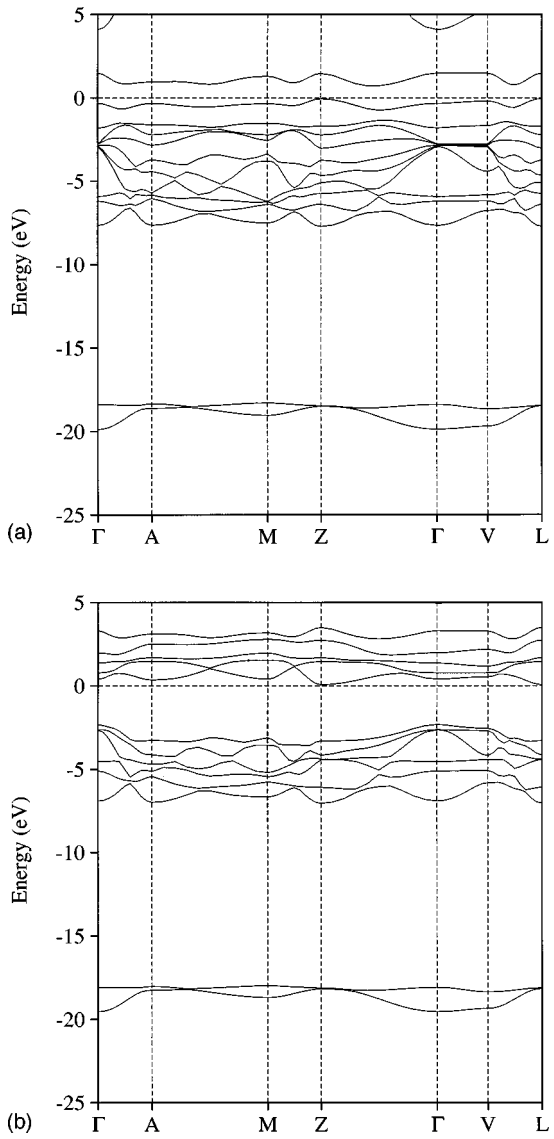

FIG. 4. The LDA energy band structures of $LiMnO_2$ in the monoclinic structure (a) for the majority spin and (b) for the minority spin.

through Eq. (1). Potentials in the different structures with and without magnetic effects are listed in Table VI for the LDA approximation and in Table VII for the GGA approximation. In the LDA (Table VI), spin polarization has a substantial effect on the Li potential. Oddly, the change from non-spin-polarized to spin polarized is not in the same direction for the different structures. While the Li potential in the layered and spinel structure decreases with spin-polarization by about 0.3 V, the potential of the orthorhombic phase increases by a similar amount. The Li potential for the spinel $LiMn_2O_4/Li_2Mn_2O_4$ couple is reduced dramatically with spin polarization due to the strongly increased stability of spinel $LiMn_2O_4$. In the GGA (Table VII) these trends mostly continue.

IV. DISCUSSION

Our results indicate that the relative stability of structures in the Li_xMnO_2 system is strongly influenced by the magnetic state of the material. For $LiMnO_2$ the coupling between the magnetic state and the Jahn-Teller distortion around the Mn^{3+} ion further complicates the physics of this material.

(a) *Composition* MnO_2. While we find that the layered form has the lowest energy among the structures we tried (with spin-polarized LDA), this result cannot be verified directly as experimentally the β-MnO_2 structure is believed to be stable.[40,41] We did not consider this structure in our analysis. Only ferromagnetic calculations were performed although the system is likely antiferromagnetic due to the very short bonds between the Mn^{4+} cations.[38]

(b) *Composition* $LiMn_2O_4$. The fact that spinel $LiMn_2O_4$ is highly stable in this system is not surprising and well documented by experiments. Antiferromagnetism is found to be stable, in agreement with experiments.[38] Because the average valence of Mn is 3.5, only half of the oxygen octahedra will be JT distorted if the charge on Mn disproportionates to $+3$ and $+4$. The unit cell and space group suggested experimentally[9,42] does not allow for such disproportionation

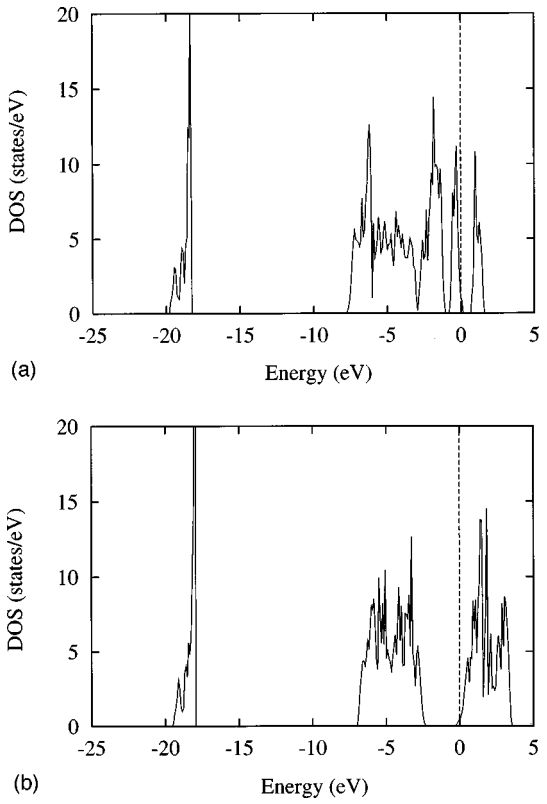

FIG. 5. The LDA one electron density of states (DOS) of $Li_2Mn_2O_4$ in the lithiated tetragonal spinel structure (a) for the majority spin and (b) for the minority spin.

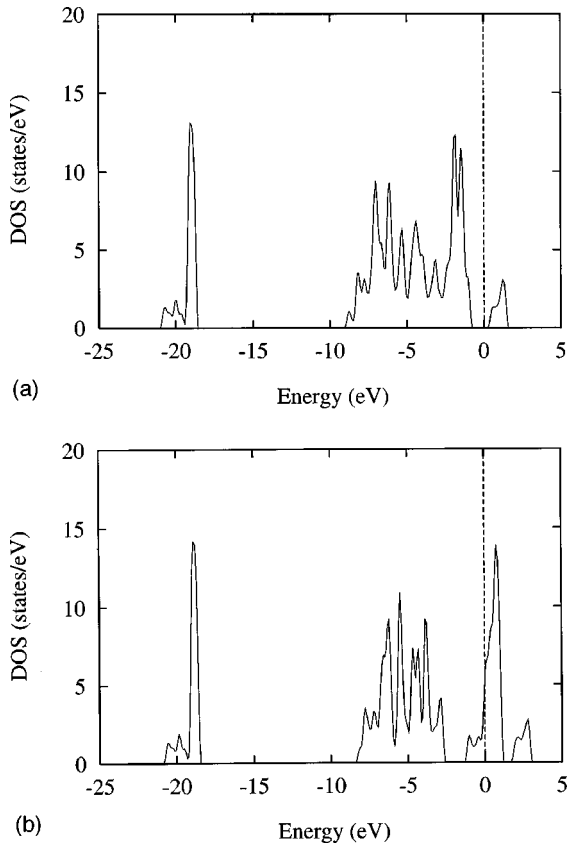

FIG. 6. The LDA one electron density of states (DOS) of $LiMn_2O_4$ in the lithiated cubic spinel structure (a) for the majority spin and (b) for the minority spin.

as it requires all Mn ions to be equivalent. It is therefore not surprising that in our calculation, based on the $I4_1/amd(D_{4h})$ symmetry, we do not find the tetragonal distortion. Indirect evidence for nonequivalent Mn ions comes from EXAFS data obtained by Yamaguchi *et al.*[13] who found that some oxygen octahedra are clearly JT distorted as they split the Mn-O distances in a set of 4 and 2. Very recently Carvajal *et al.*[14] proposed an unit cell in which Mn^{3+} and Mn^{4+} are both present.

(c) *Composition* $LiMnO_2$. At composition $LiMnO_2$, the manganese ion has formal valence $3+$ and the effects of magnetism and the choice of exchange correlation function are most subtle. With no magnetic moment on Mn ions [in non-spin-polarized LDA, Fig. 1(a)] the undistorted layered structure is stable. This is actually the structure one would expect for $LiMnO_2$ based on ionic size considerations.[43,44] The ionic radius of high spin Mn^{3+} ion in octahedral environment is 0.645 Å.[45] Typically, the layered structure is stabilized in alkali-transition-metal dioxides when the ratio of the transition metal radius to alkali radius is less than about 0.9.[43,44] The ionic radius of Li^+ is 0.76 Å.[45] While ferromagnetic spin polarization (within the LDA) clearly brings the orthorhombic and spinel based phases closer in energy to the layered structure, the latter remains stable.

With spin-polarized LDA, only *metastable* JT distortions could be obtained. Figure 1(b) shows that the undistorted layered (LA) and cubic spinel (SPC) are actually lower in energy than their deformed counterparts (MLA and SPT, respectively). Although antiferromagnetic LDA calculations bring the energy of the deformed structures down somewhat, the ferromagnetic undeformed structures remain lowest in energy.

It is interesting to note that the relative magnitude of the Jahn-Teller distortion as measured by the largest difference in nearest neighbor manganese-oxygen distance divided by the average Mn-O bond length, is around 19% for the spin polarized LDA, in striking agreement with the experimental values measured for the monoclinic layered and lithiated spinel structures. This seems to imply that the JT distortion by itself is not sufficient to stabilize the deformed structures. The absence of stable JT distortions has been reported before with the LDA approximation.[46] In perovskite manganese oxide ($LaMnO_3$) the JT distortion has been investigated using the LDA, GGA, and LDA+U method. Within LDA and GGA, the structure of $LaMnO_3$, when relaxed, becomes nearly cubic and the JT distortion is significantly suppressed. Even the LDA+U method was found to underestimate the JT distortion in this material. The fact that increasing the volume by applying negative pressure in the LDA calculations helps to stabilize the Jahn-Teller distortion can be easily understood. A large volume will reduce the e_g band width and the elastic energy cost of the Jahn-Teller distortion. Both effects will enhance the distortion.

Only in the GGA approximation (Fig. 2 and Table V) is the relative stability of various structures acceptable. Ferromagnetic GGA calculations make the JT deformed MLA structure stable over the LA structure by 248 meV. Although we did not calculate the ferromagnetic tetragonal spinel in this approximation we expect that it would also be stable

TABLE VI. The average open-cell voltages in V calculated with LDA for non-spin-polarized (NSP) and spin polarized (SP) cases in various structures, namely, layered (LA), cubic spinel (SPC), and orthorhombic (ORTHO).

	Structure	$MnO_2/LiMnO_2$	$Mn_2O_4/LiMn_2O_4$	$LiMn_2O_4/Li_2Mn_2O_4$
	LA	3.31		
NSP	ORTHO	2.78		
	SPC	3.24	3.85(4.10)	2.63(2.7)
	LA	2.95		
SP	ORTHO	3.06		
	SPC	2.94	3.95(4.10)	1.93(2.7)

over its cubic counterpart. However, even ferromagnetic GGA calculations do not predict the correct ground state as they put the ferromagnetic MLA some 8 meV below the orthorhombic structure. To obtain the latter as ground state, antiferromagnetic spin ordering is required. For the spin configurations described earlier ORTHO is stable over MLA by 32 meV.

The comparison between the LDA and GGA results points towards the importance of charge localization. In the GGA charge gradients tend to be more pronounced than in LDA. The resulting charge localization seems essential to obtain stable JT distortions (as compared to metastable ones in the LDA).

Stable antiferromagnetism is to be expected in these oxides as they have relatively low Mn-Mn distances. Antiferromagnetism (AF) is induced by the direct overlap of half filled orbitals in the Mn ions.[47] In addition to the direct Mn-Mn exchange, the superexchange is mostly of the 90° type and largely antiferromagnetic as well. The energy difference between the antiferromagnetic and ferromagnetic ordering is very large (-166 meV for ORTHO and -127 meV for MLA). This difference is considerably larger than the values obtained with unrestricted Hartree Fock on the experimental geometries.[39] The effect of antiferromagnetism on the *relative* stability of structures (e.g., MLA and ORTHO) is more difficult to explain. The antiferromagnetic configurations used for both structures are very similar. They both have AF chains along the shortest Mn-Mn bonds. The interchain interaction is along longer bonds and cancels out due to frustration (i.e., an identical number of antiferromagnetic and ferromagnetic bonds exists between the chains). The only significant difference may be the more three dimensional nature of the spin ordering in the orthorhombic structure. In this structure, there is interchain interaction not only along the *c* axis (direct Mn-Mn), but also along the *b* axis through a 180° superexchange (the actual bond angle is about 170°). The two-dimensional Li-Mn ordering of the MLA structure prohibits these interplain couplings.

The band structures of the lithiated manganese oxides are fairly typical. They show the expected splitting of the metal-derived bands into a lower t_{2g} and upper e_g complex. For structures with no Jahn-Teller distortion the splitting of those two sets of bands is too large for Mn^{3+} to be completely high spin and the last valence electron pairs with an electron with opposite spin in the t_{2g} bands [see Fig. 3(b)]. For the JT distorted structures (MLA: Fig. 4 and SPT: Fig. 5) one of the e_g band is pushed down below the Fermi level allowing the Mn^{3+} ion to become fully spin polarized. The higher magnetic moment of the Mn^{3+} ion in the deformed structure explains why their stability benefits from the appropriate spin ordering.

Several implications for practical Li-intercalation oxides can be deduced from the results. Clearly, the spinel $LiMn_2O_4$ is highly stable. Its formation energy in the GGA approximation is almost 0.5 eV. This may explain why, when the Li content of orthorhombic and monoclinic layered $LiMnO_2$, is reduced by electrochemical reaction in a battery, both transform to the spinel structure.[24,48,49] We found that the spinel structure is also stable in most other $3d$ lithium-transition metal oxides, although none of them has as large a formation energy than $LiMn_2O_4$.[50]

The average Li-intercalation potentials in Tables VI and VII show fair to good agreement with experiment, although a consistent underprediction occurs. This was already observed in previous calculations on a large number of transition-

TABLE VII. The average open-cell voltages in V calculated with GGA for spin polarized case in various structures, namely, layered (LA), monoclinic layered (MLA), cubic spinel (SPC), tetragonal spinel (SPT), and orthorhombic (ORTHO). AF energies were used at all compositions except at the MnO_2 composition where the FM energy was taken into account.

Structure	$MnO_2/LiMnO_2$	$Mn_2O_4/LiMn_2O_4$	$LiMn_2O_4/Li_2Mn_2O_4$
LA	2.58		
MLA	2.95		
ORTHO	3.32		
SPC	2.86	3.62(4.10)	2.10
SPT	2.93	3.62	2.25(2.7)

metal oxides.[51,52] The substantial error for the $LiMn_2O_4$/$Li_2Mn_2O_4$ couple could be related to the fact that the experimentally observed structure has somewhat different site occupancy than the one used in the calculations. In addition, the energy of $LiMn_2O_4$ represents a system with no JT distortions. Recent experimental evidence indicates that local JT distortion can still exist even when there is no distortion of the cell.[13] This effect may also contribute to the error in the intercalation potential.

V. CONCLUSION

We have presented a series of LDA and GGA calculations with ferro and antiferromagnetic spin ordering for lithiated manganese oxides. Due to the large magnetic moment on the mangenese ions, spin polarization has a significant effect on the energies and relative stability of various structures. The level of exchange-correlation correction as well as the spin ordering are found to be essential for reproducing the correct ground state at composition $LiMnO_2$. Globally stable JT distortion could only be obtained within the GGA or in LDA with the use of negative pressure.

Although the Jahn-Teller distortion is important for $LiMnO_2$ structures, it does not suffice to explain their relative stability as all structures have similar JT distortions. A more appropriate view may be that the JT distortion is necessary to localize charge (i.e., into a single e_g orbital) which in turn increases the magnetic moment on the Mn ion. It is the interaction between these moments which determines the stability of orthorhombic $LiMnO_2$ over monoclinic layered $LiMnO_2$.

The realization that orthorhombic $LiMnO_2$ is stabilized over monoclinic layered $LiMnO_2$ by antiferromagnetism offers exciting possibilities for engineering the relative stability between these two structures. The layered structure is often favored as its Li diffusion constant is believed to be higher. We will report on this in a subsequent paper. For all structures at composition $LiMn_2O_4$ and $LiMnO_2$ we found stable antiferromagnetic ordering of the Mn ions. Our results also point out the potential pitfalls of using the local density approximation in these materials.

ACKNOWLEDGMENTS

We gratefully thank the San Diego Supercomputing Center for providing us with computing resources. This project was supported primarily by MRSEC Program of the National Science Foundation under Award No. DMR-9400334. We thank A. Van der Ven, Dr. M. K. Aydinol, and Dr. Dane Morgan for helpful discussions.

[1] H. Ikeda, T. Saito, and H. Tamura, in *Manganese Dioxide Symposium*, edited by A. Kozawa and R. H. Brodd (Cleveland Section of The Electrochemical Society, Princeton, NJ, 1975), Vol. 1, p. 384.
[2] J. C. Hunter, J. Solid State Chem. **39**, 142 (1981).
[3] J. B. Goodenough, M. M. Thackeray, W.I.F. David, and P.G. Bruce, Rev. Chim. Miner. **21**, 435 (1984).
[4] M. M. Thackeray, W. I. F. David, P. G. Bruce, and J. B. Goodenough, Mater. Res. Bull. **18**, 461 (1983).
[5] J. M. Tarascon, W. R. McKinnon, F. Coowar, T. N. Bowmer, G. Amatucci, and D. Guyomard, J. Electrochem. Soc. **141**, 1421 (1994).
[6] J. B. Goodenough and A. L. Loeb, Phys. Rev. **98**, 391 (1955).
[7] John B. Goodenough, Phys. Rev. **100**, 564 (1955).
[8] G. Ceder, M. K. Aydinol, and A. F. Kohan, Comput. Mater. Sci. **8**, 161 (1997).
[9] Atsuo Yamada and Masahiro Tanaka, Mater. Res. Bull. **30**, 715 (1995).
[10] A. Yamada, J. Solid State Chem. **122**, 160 (1996).
[11] A. Yamada, K. Miura, K. Hinokuma, and M. Tanaka, J. Electrochem. Soc. **142**, 2149 (1995).
[12] J. Sugiyama, T. Atsumi, A. Koiwai, T. Sasaki, T. Hioki, S. Noda, and N. Kamegashira, J. Phys.: Condens. Matter **9**, 1729 (1997).
[13] H. Yamaguchi, A. Yamada, and H. Uwe, Phys. Rev. B **58**, 8 (1998).
[14] J. Rodriguez-Carvajal, G. Rousse, C. Masquelier, and M. Hrvieu, Phys. Rev. Lett. **81**, 4660 (1998).
[15] K. Kanamura, H. Naito, T. Yao, and Z. Takehara, J. Mater. Chem. **6**, 33 (1996).
[16] G. Rousse, C. Masquelier, J. Rodriguez-Carvajal, and M. Hervieu, Electrochem. Solid-State Lett. **2**, 6 (1999).
[17] J. E. Greedan, N. P. Raju, and I. J. Davidson, J. Solid State Chem. **128**, 209 (1997).
[18] L. Croguennec, P. Deniard, and R. Brec, J. Electrochem. Soc. **144**, 3323 (1997).
[19] G. Dittrich and R. Hoppe, Z. Anorg. Allg. Chem. **368**, 262 (1969).
[20] R. Hoppe, G. Brachtel, and M. Jansen, Z. Anorg. Allg. Chem. **417**, 1 (1975).
[21] W. I. F. David, M. M. Thackeray, L. A. de Picciotto, and J. B. Goodenough, J. Solid State Chem. **67**, 316 (1987).
[22] A. Robert Armstrong and Peter G. Bruce, Nature (London) **381**, 499 (1996).
[23] F. Capitaine, P. Gravereau, and C. Delmas, Solid State Ionics **89**, 197 (1996).
[24] G. Vitins and K. West, J. Electrochem. Soc. **144**, 2587 (1997).
[25] Mitsuharu Tabuchi, Kazuaki Ado, Hironori Kobayashi, Hiroyuki Kageyama, Christian Masquelier, Atsuro Kondo, and Ryoji Kanno, J. Electrochem. Soc. **145**, L49 (1998).
[26] Young-Il Jang, Biying Huang, Yet-Ming Chiang, and Donald R. Sadoway, Electrochem. Solid State Lett. **1**, 13 (1998).
[27] G. Kresse and J. Furthmuller, Comput. Mater. Sci. **6**, 15 (1996).
[28] G. Kresse and J. Furthmuller, Phys. Rev. B **54**, 11 169 (1996).
[29] G. Kresse and J. Hafner, Phys. Rev. B **49**, 14 251 (1994).
[30] M. K. Aydinol and G. Ceder, J. Electrochem. Soc. **144**, 3832 (1997).
[31] M. K. Aydinol, A. F. Kohan, G. Ceder, K. Cho, and J. Joannopoulos, Phys. Rev. B **56**, 1354 (1997).
[32] G. Ceder, Y.-M. Chiang, D. R. Sadoway, M. K. Aydinol, Y.-I. Jang, and B. Huang, Nature (London) **392**, 694 (1998).
[33] A. Van der Ven, M. K. Aydinol, and G. Ceder, G. Kresse, and J. Hafner, Phys. Rev. B **58**, 2975 (1998).
[34] R. Benedek and M. M. Thackeray, Phys. Rev. B **56**, 10 707 (1997).
[35] C. Wolverton and A. Zunger, Phys. Rev. B **57**, 2242 (1998).

[36] E. Deiss, A. Wokaun, J.-L. Barras, C. Daul, and P. Dufek, J. Electrochem. Soc. **144**, 3877 (1997).
[37] D. J. Singh, Phys. Rev. B **55**, 309 (1997).
[38] C. Masquelier, M. Tabuchi, K. Ado, R. Kanno, Y. Kobayashi, Y. Maki, O. Nakamura, and J. B. Goodenough, J. Solid State Chem. **123**, 255 (1996).
[39] W. C. Mackrodt and E.-A. Williamson, Philos. Mag. B **77**, 1077 (1998).
[40] Cyrus Klingsberg and Rustum Roy, J. Am. Ceram. Soc. **43**, 623 (1960).
[41] H. Hino, T. Minato, and Y. Kusakabe, Mem. Fac. Eng., Kyoto Univ. **40**, 16 (1978).
[42] T. Ohzuku, M. Kitagawa, and T. Hirai, J. Electrochem. Soc. **137**, 769 (1990).
[43] Eric J. Wu, Patrick D. Tepesch, and Gerbrand Ceder, Philos. Mag. B **77**, 1039 (1998).
[44] T. A. Hewston and B. L. Chamberland, J. Phys. Chem. Solids **48**, 97 (1987).
[45] R. Shannon, Acta Crystallogr., Sect. A: Cryst. Phys., Diffr., Theor. Gen. Crystallogr. **32**, 751 (1976).
[46] H. Sawada, Y. Morikawa, K. Terakura, and N. Hamada, Phys. Rev. B **56**, 12 154 (1997).
[47] J. B. Goodenough, *Magnetism and the Chemical Bond* (Wiley, New York, 1963).
[48] I. J. Davidson, R. S. McMillan, J. J. Murray, and J. E. Greedan, J. Power Sources **54**, 232 (1995).
[49] I. Koetschau, M. N. Richard, J. R. Dahn, J. B. Soupart, and J. C. Rousche, J. Electrochem. Soc. **142**, 2906 (1995).
[50] A. Van der Ven (private communication).
[51] G. Ceder, Science **280**, 1099 (1998).
[52] G. Ceder, A. Van der Ven, and M. K. Aydinol, JOM **50**, 35 (1998).